

RESEARCH

Open Access



# Experimentally designed electrochemical sensor for therapeutic drug monitoring of Ondansetron co-administered with chemotherapeutic drugs

Mona A. Abdel Rahman<sup>1</sup>, Shima A. Atty<sup>2</sup>, Sally S. El-Mosallamy<sup>3\*</sup>, Mohamed R. Elghobashy<sup>3,1</sup>, Hala E. Zaazaa<sup>3</sup> and Ahmed S. Saad<sup>3,4</sup>

## Abstract

The experimental design extracts valuable information about the main effects and interactions from the least number of experiments. The current work constructs a solid-state sensor for selective assay of Ondansetron (OND) in pharmaceutical dosage form and plasma samples. During optimization, the Design Expert<sup>®</sup> statistical package constructed a custom design of 15 sensors with different recipes. We fed the software with the experimentally observed performance parameters for each sensor (slope, LOQ, correlation coefficient, and selectivity coefficient for sodium ions). The computer software analyzed the results to construct a prediction model for each response. The desirability function was adjusted to optimize the Nernstian slope, minimize the LOQ and selectivity coefficients, and maximize the correlation coefficient (*r*). The practical responses of the optimized sensor were close to those predicted by the model (slope = 60.23 mV/decade slope, LOQ =  $9.09 \times 10^{-6}$  M, *r* = 0.999, sodium selectivity coefficient =  $1.09 \times 10^{-3}$ ). The sensor successfully recovered OND spiked to tablets and human plasma samples with mean percentage recoveries of  $100.01 \pm 1.082$  and  $98.26 \pm 2.227$ , respectively. Results were statistically comparable to those obtained by the reference chromatographic method. The validated potentiometric method can be used for fast and direct therapeutic drug monitoring of OND co-administered with chemotherapeutic drugs in plasma samples.

**Keywords:** Design of experiment, Potentiometric sensor, Ondansetron assay, Therapeutic drug monitoring, Plasma

## Introduction

With rising global competitiveness and the expanding effect of information technology, the pharmaceutical sector urgently needs to enhance its operational efficiency and increase product quality. Pharmaceutical companies restructured and standardized the Quality-by-Design (QbD) approach to satisfy customer needs and achieve quality in the operation process and excellence in the

market [1]. In the pharmaceutical industry, the QbD is a systematic approach that defines objectives and understands the sources of variability to control the product and process. In its Q8 and Q11 guidelines, the International Conference on Harmonization (ICH) has recently mentioned the QbD and its application in the pharmaceutical industry. The QbD in analytical method development —also known as Analytical Quality by Design (AQbD)—represents a leap that achieves the desired method performance. In a few words, the QbD's primary focus is to maximize productivity and quality and minimize risk. The design of experiments (DoE) is a vital part of QbD. DoE uses a limited number of experiments

\*Correspondence: sally.el-mosallamy@pharma.cu.edu.eg

<sup>3</sup> Analytical Chemistry Department, Faculty of Pharmacy, Cairo University, Kasr El-Aini St, PO 11562, Cairo, Egypt

Full list of author information is available at the end of the article



© The Author(s) 2022. **Open Access** This article is licensed under a Creative Commons Attribution 4.0 International License, which permits use, sharing, adaptation, distribution and reproduction in any medium or format, as long as you give appropriate credit to the original author(s) and the source, provide a link to the Creative Commons licence, and indicate if changes were made. The images or other third party material in this article are included in the article's Creative Commons licence, unless indicated otherwise in a credit line to the material. If material is not included in the article's Creative Commons licence and your intended use is not permitted by statutory regulation or exceeds the permitted use, you will need to obtain permission directly from the copyright holder. To view a copy of this licence, visit <http://creativecommons.org/licenses/by/4.0/>. The Creative Commons Public Domain Dedication waiver (<http://creativecommons.org/publicdomain/zero/1.0/>) applies to the data made available in this article, unless otherwise stated in a credit line to the data.

to identify the critical method variables based on statistical significance testing. It determines the optimum range for each variable to achieve the desired analytical performance with acceptable robustness [2–4]. Cancer is the uncontrollable growth and dissemination of abnormal cells throughout the body [5]. Cancer is the world's second most common cause of death, killing more than 8 million people annually; cancer incidence is predicted to rise by more than 50% in the coming decades [6, 7].

Chemotherapeutic agents are used individually or in combination to treat different cancer types. However, it risks emetogenic side effects such as nausea and vomiting [8]. The control of such side effects is crucial for effective treatment and patient compliance. Ondansetron (OND), a type 3 serotonin (5-HT<sub>3</sub>) receptor antagonist in the brain and GIT, is the first-line treatment for the emetogenic side effects of chemotherapy [9]. OND is chemically known as (RS)-9-methyl-3-[(2-methyl-1H-imidazole-1-yl) methyl]-2,3-dihydro-1H-carbazol-4(9H)-one. It is a basic compound ( $pK_a$  of 7.34) highly soluble in acidic media and sparingly solubility in water [10]. It treats nausea and vomiting during chemotherapy, radiotherapy, anxiolytic, and neuroleptic problems. The 5-HT<sub>3</sub> released during chemotherapy, radiotherapy, and surgery stimulate the 5-HT<sub>3</sub> receptors in the chemoreceptor trigger zone that sends signals to the vomiting center in the brain [11–13].

Cytochrome P-450 enzymes (including the polymorphic CYP2D6 and CYP1A2) are involved in the biotransformation of OND, leading to a significant intra-individual variation in OND plasma concentrations and thus its efficacy [14]. Therefore, it was mandatory to develop a real-time analytical method for the rapid, sensitive, and selective assay of OND to adjust its dose during chemotherapy.

British Pharmacopoeia reports non-aqueous titrimetric and HPLC methods [15] for OND. The literature reported additional spectrofluorimetry [16], spectrophotometry [17–23], voltammetry [24, 25], radioimmunoassay [26], flow injection [27, 28], thin-layer chromatography [29, 30], high-performance liquid chromatography [31–41], and liquid chromatography-tandem mass spectrometry (LC–MS/MS) [42, 43]. The discussed methods come at a high expense and call for laboratories that are well-equipped. Thus, the aforementioned techniques did not fit routine analysis because they involved a lengthy analysis time, a complex instrument setup, and multiple manipulation steps. Ion-selective electrode-potentiometry is a low-cost, economical, simple-to-use, and non-destructive technique. Ion-selective electrodes (ISEs) enable continuous monitoring of minimal sample volume

without sample pretreatment. They are also suitable for colored or cloudy samples [44, 45]. A single potentiometric method was reported for OND determination [46]. However, the current OND sensor was the first to use the QbD approach to reach the target analytical response.

The current work aims to develop an ion-selective electrode potentiometric sensor for the therapeutic drug monitoring of OND in plasma samples and routine analysis in quality control laboratories. The mentioned objective demands a rapid, sensitive, and selective sensor response with minimal sample treatment. The sensor development followed a QbD approach to reach the desired analytical goal. Based on our recently published work [47], we identified the critical sensor variables and the response parameters that have to be monitored to achieve the desired analytical objective.

## Experimental

### Apparatus

Potential measurements were performed utilizing a digital potentiometer, Jenway model 3330 (Essex, UK), with a double junction Ag/AgCl reference electrode, Orion, ThermoScientific no. 900200, and a magnetic stirrer, Bandelin Sonoro, R510S (Budapest, Hungary), and a Jenway (924051, UK) glass electrode were used.

### Reagents, reference standards and materials

Analytical-grade chemicals were employed in this study. Poly(vinyl)chloride (PVC), Nitrophenyl octyl ether (NPOE), and dioctyl phthalate (DOP) were purchased from Alfa-Aesar (Ward Hill, MA, USA). Phosphotungstic acid (PT), phosphomolybdic acid (PM), sodium tetraphenylborate (TPB), tetrakis (TKS), ammonium Reineckate (RK), carboxymethyl- $\beta$ -cyclodextrin (CMBCD), hydroxypropyl- $\beta$ -cyclodextrin (HPBCD), calix-[8]-arene (CX<sub>8</sub>), calix-[4]-arene (CX<sub>4</sub>), and tetrahydrofuran (THF) were purchased from Aldrich (Steinheim, Germany). Potassium dihydrogen phosphate, sodium hydroxide, hydrochloric acid, and metal salts were purchased from El-NASR Pharmaceutical Chemical Co., Abu-Zabaal, Cairo, Egypt, as chlorides. Phosphate buffer pH 5.5 was prepared by adjusting the pH of  $1 \times 10^{-3}$  M potassium dihydrogen phosphate solution (using bi-distilled water as solvent) to pH 5.5 with 1 M NaOH solutions. Ondansetron working standard (99.87% purity) was obtained from Sigma-Aldrich (St. Louis, MO, USA). Zofran<sup>®</sup> tablet (Batch no: B74319 C) containing 8.0 mg OND; was purchased from the local market. Plasma samples were obtained from Vacsera Co. (Giza, Egypt).

Stock standard solution ( $1.0 \times 10^{-2}$  M) OND was prepared in phosphate buffer pH 5.5. Serial dilutions of the

stock standard solution were carried out to prepare OND working standard solutions in the range  $1.00 \times 10^{-6}$  to  $1.0 \times 10^{-3}$  M using phosphate buffer pH 5.5 as a solvent.

## Procedure

### Optimization of the PVC membrane composition

**Custom experimental design** We adopted a custom experimental design that included three categorical factors: plasticizer, ion exchanger, and ionophore types. The design included 15 sensors with two levels for the plasticizer type (NPOE and DOP), five levels for the ion-exchanger type (TPB, PT, PM, TKS, RK). and five levels for the ionophore types (BCD, HPBCD, CMBCD, CX<sub>4</sub>, CX<sub>8</sub>) levels were coded as shown in Table 1.

The slope (S), correlation coefficient (r), the negative logarithm of the quantification limit (pLOQ), and the selectivity coefficient for sodium ions ( $\log K_{\text{OND,Na}^+}^{\text{pot}}$ ) were recorded for each of the 15 sensors (Table 1). The experiments evaluated the main effects and interactions between the three studied factors. We adjusted the desirability function to achieve the optimum slope and maximum pLOQ and r, and minimum  $\log K_{\text{OND,Na}^+}^{\text{pot}}$ .

**Membrane fabrication and sensor assembly** Solutions of the membrane components were separately prepared by transferring accurate weights of each component, including PVC, plasticizer (NPOE and DOP), ion-exchanger (TPB, PT, PM, TKS, RK), and ionophore (BCD, HPBCD, CMBCD, CX<sub>4</sub>, CX<sub>8</sub>) in a tube and dissolve it in an adequate amount of THF. The membrane recipes were pre-

pared by mixing accurate volumes of the prepared solutions as described in Table 1. A micropipette was used to drop cast an accurate volume of the membrane component over the coated glassy carbon electrode surface electrochemically coated with polyaniline [48], then left to dry at room temperature.

**Sensor calibration** The potential differences were measured between the working and the reference electrode immersed in OND solutions ( $1.00 \times 10^{-6}$  to  $1.0 \times 10^{-2}$  M) and stirred at 100 rpm until a stable response was reached within  $\pm 1.0$  mV. The sensor was then washed with distilled water before measuring the potential differences. Similarly, calibrations were held in human plasma samples after ten-fold dilution with phosphate buffer. The regression equations were computed for each sensor by plotting the potential against the logarithm of the molar concentration. Slopes, correlation coefficients, and limits of quantification were calculated.

**Effect of pH** The optimized sensor was used to monitor the difference in potential when pH is deliberately changed in  $1.0 \times 10^{-2}$  M and  $1.0 \times 10^{-3}$  M solutions of OND. The change in pH was done by adding a small amount of aqueous 0.1 M NaOH and 0.1 M HCl. The potential and pH were recorded after each addition and plotted against one another to obtain the pH curve.

**Stability of the proposed sensor** The potential difference between the optimized sensor and the ref-

**Table 1** The custom experimental design architecture for the levels and components of the studied sensors and the observed responses for each sensor

Sensor no	Factor 1		Factor 2		Factor 3		Response 1	Response 2	Response 3	Response 4
	Plasticizer		Ion exchanger		Ionophore		Slope	r	pLOQ	$\log K_{\text{OND,Na}^+}^{\text{pot}}$
1	-1	NPOE	2	RK	-2	BCD	53.55	0.9984	4.57	-2.50
2	1	DOP	2	RK	-1	HPBCD	53.10	0.9992	4.57	-3.71
3	-1	NPOE	-1	PT	-1	HPBCD	62.79	0.9983	4.36	-4.22
4	-1	NPOE	1	TKS	1	CX <sub>4</sub>	59.70	0.9972	5.32	-2.96
5	1	DOP	-1	PT	0	CMBCD	62.56	0.9986	4.79	-3.44
6	1	DOP	1	TKS	2	CX <sub>8</sub>	56.49	0.9976	5.03	-3.56
7	-1	NPOE	0	PM	-1	HPBCD	59.05	0.9980	4.01	-4.23
8	-1	NPOE	-2	TPB	2	CX <sub>8</sub>	59.05	0.9965	4.57	-2.11
9	-1	NPOE	-1	PT	-2	BCD	66.41	0.9988	5.04	-2.88
10	1	DOP	-1	TPB	-2	BCD	60.78	0.9960	5.04	-2.86
11	-1	NPOE	2	RK	2	CX <sub>8</sub>	59.05	0.9981	4.57	-2.96
12	-1	NPOE	0	PM	0	CMBCD	56.04	0.9994	4.52	-3.12
13	-1	NPOE	1	TKS	0	CMBCD	60.15	0.9980	5.04	-2.94
14	-1	NPOE	-2	TPB	1	CX <sub>4</sub>	66.75	0.9971	5.32	-2.25
15	1	DOP	0	PM	1	CX <sub>4</sub>	50.25	0.9986	4.97	-3.26

reference electrode was recorded in OND solutions ( $2.68 \times 10^{-5}$ – $4.07 \times 10^{-4}$  M). The time required to reach a stable response within one mV from the equilibrium potential was recorded.

**Sensor selectivity** The IUPAC's Separate Solutions Method (SSM) [49] was used to calculate the potentiometric selectivity coefficient  $K_{\text{OND,Int}}^{\text{pot}}$  for different cationic contaminants ( $\text{K}^+$ ,  $\text{Na}^+$ ,  $\text{NH}_4^+$ ,  $\text{Ca}^{2+}$ ,  $\text{Mg}^{2+}$ ,  $\text{Cd}^{2+}$ ,  $\text{Fe}^{2+}$ , and  $\text{Cr}^{3+}$ ). Measurements were performed in  $1.0 \times 10^{-3}$  M solutions of OND and the interfering cations, and the selectivity coefficient was calculated according to the Nicolsky–Eisenman equation [50].

$$\log k_{\text{OND,Int}}^{\text{pot}} = \frac{E_{\text{Int}} - E_{\text{OND}}}{S} + \left(1 - \frac{z_{\text{OND}}}{z_{\text{Int}}}\right) \log a_{\text{OND}} \quad (1)$$

where  $K_{\text{OND,Int}}^{\text{Pot}}$  the selectivity coefficient,  $E_{\text{OND}}$  and  $E_{\text{Int}}$  represent the potential of OND and interfering ions, respectively,  $z_{\text{OND}}$  and  $z_{\text{Int}}$  refer to the charge of OND and the interfering ions, respectively,  $S$  is the calibration curve slope, and  $a_{\text{OND}}$  the OND concentration.

**Sensor reversibility** The reproducibility was evaluated by reciprocally dipping the optimized sensor and the reference electrode in two different OND solutions ( $1.0 \times 10^{-4}$  M and  $1.0 \times 10^{-3}$  M).

### Application

**Assay of OND in Zofran® tablets** The average weight of one Zofran® tablet was determined from the uniform powder of five crushed tablets. The powder was transferred into a 50 mL measuring flask and sonicated with 30 mL phosphate buffer (pH 5.5) for 15.0 min, and the volume was then completed using the same solvent. The solution was diluted ten times before measuring the potential difference between the optimized sensor and the reference electrode before and after adding 1 mL of OND stock standard solution  $1 \times 10^{-2}$  M. The sample concentration ( $C_x$ ) was calculated from the standard addition equation [51]:

$$C_x = C_s \left( \frac{V_s}{V_x + V_s} \right) \left[ 10^{n(\Delta E/S)} - \frac{V_x}{V_s + V_x} \right]^{-1} \quad (2)$$

where  $C_x$  is the concentration in the sample solution,  $V_x$  is the sample solution volume,  $C_s$  and  $V_s$  are the concentration and volume, respectively, of added standard solution,  $\Delta E$  is the change in potential after standard addition, and  $S$  stands for the slope of the calibration curve in mV per decade.

**Assay of spiked plasma samples** Human plasma samples (450  $\mu\text{L}$ ) were transferred into a 5 mL measuring

flask and spiked with 50  $\mu\text{L}$  of OND standard solutions ( $1.0 \times 10^{-2}$ – $1.0 \times 10^{-3}$  M). The volume was completed to the mark using the phosphate buffer. The previously mentioned standard addition technique was followed to determine OND concentration in the spiked plasma samples.

## Results and discussion

The quality by design approach was applied to develop a potentiometric method that fits for definite analytical purposes. The study employed the design expert program to (1) develop a custom experimental design, (2) analyze the results to evaluate the effect of the studied factors, and (3) build a prediction model that serves to (4) optimize the sensor composition according to the desired analytical performance and intended analytical purposes.

### Optimization study

The sensor performance is a function of its composition and assembly; a properly selected membrane recipe will inevitably lead to the desired performance [52]. We developed an optimization study to evaluate the significance and quantified the main effects and interactions among the studied factors (plasticizer, ion exchanger, and ionophore) (Table 1). The study included two plasticizers (NPOE, DOP), five ion exchangers (TPB, PT, PM, TKS, RK), and five ionophores (BCD, HPBCD, CMBCD, CX<sub>4</sub>, CX<sub>8</sub>). The measured outcomes included the slope, correlation coefficient, quantification limit, and sodium selectivity as descriptors for the method performance; the results were statistically analyzed using One-Way ANOVA (Table 2).

We measured outcomes that serve the desired analytical objective. An ideal sensor produces a stable Nernstian slope, maximum correlation coefficient, minimal quantification limit, and minimal sodium selectivity coefficient. Finally, we used the prediction model to select the levels of each factor that can achieve the defined method objective. The defined outcomes were calculated according to the IUPAC recommendations [49].

The Design Expert® was fed with the practically estimated outcomes for each studied sensor. The program analyzed each of the four responses to build a separate prediction model for each. The prediction models were statistically analyzed using the One-way ANOVA test to determine the significance of the prediction model and the factors that significantly affect each outcome. We decided to use the pLOQ instead of the LOQ directly to minimize decimal places. Therefore, it is desired to maximize the pLOQ for better sensor performance. One-way ANOVA proved the ability of the model to predict the sensor slope, correlation coefficient, pLOQ, and sodium selectivity ( $p < 0.05$ ).

**Table 2** The One-way ANOVA analysis of the estimated performance parameters

	Source	Sum of squares	df	Mean square	F-value	p-value	
A.Slope	Model	234.84	5	46.97	6.19	0.0093	Significant <sup>a</sup>
	A-PS	43.63	1	43.63	5.75	0.0400	
	B-IE	191.20	4	47.80	6.30	0.0106	
	Residual	68.26	9	7.58			
	Cor Total	303.10	14				
B.Correlation Coefficient	Model	0.0000	4	2.548E-06	9.48	0.0020	Significant <sup>a</sup>
	B-IE	0.0000	4	2.548E-06	9.48	0.0020	
	Residual	2.687E-06	10	2.687E-07			
	Cor Total	0.0000	14				
C.pLOQ	Model	1.76	9	0.1950	6.83	0.0239	Significant <sup>a</sup>
	A-PS	0.0730	1	0.0730	2.56	0.1708	
	B-IE	0.4495	4	0.1124	3.93	0.0827	
	C-IP	0.8236	4	0.2059	7.21	0.0263	
	Residual	0.1428	5	0.0286			
	Cor Total	1.90	14				
D.logK <sub>OND,Na<sup>+</sup></sub> <sup>pot</sup>	Model	3.48	4	0.8693	4.35	0.0270	Significant <sup>a</sup>
	C-IP	3.48	4	0.8693	4.35	0.0270	
	Residual	2.00	10	0.1996			
	Cor Total	5.47	14				

<sup>a</sup> at significance level  $\alpha=0.05$

We used the One-Way ANOVA to estimate the factors that significantly affect the prediction of each of the estimated outcomes. The plasticizer ( $p=0.0400$ ) and ion-exchanger ( $p=0.0106$ ) significantly affect the slope prediction model. While the type of ion exchanger used ( $p=0.0020$ ) significantly affects the correlation coefficient prediction model. The ionophore ( $p=0.0263$ ) significantly influences the pLOQ prediction model. The ionophore ( $p=0.0270$ ) significantly affects the sodium selectivity prediction model, (Table 2).

We studied the plasticizer at two different levels (NPOE and DOP). ANOVA results proved a significant effect for the type of plasticizer on the slope. The plasticizer determines membrane properties such as polarity and conductivity. In addition, it regulates membrane conductivity by controlling the mobility of the membrane components. It modulates the membrane polarity, thus affecting selectivity and partitioning at the membrane solution interface, exudation of membrane components, and deposition of plasma proteins [53].

We studied five different levels of the ion-exchanger (TPB, PT, PM, TKS, RK). The ANOVA test proved the ion exchanger type's significant effect on the slope and correlation coefficient (Table 2). The ion exchanger modifies the membrane properties and affects the analyte exchange at the membrane solution interface. The lipophilic ion exchanger controls the membrane conductivity,

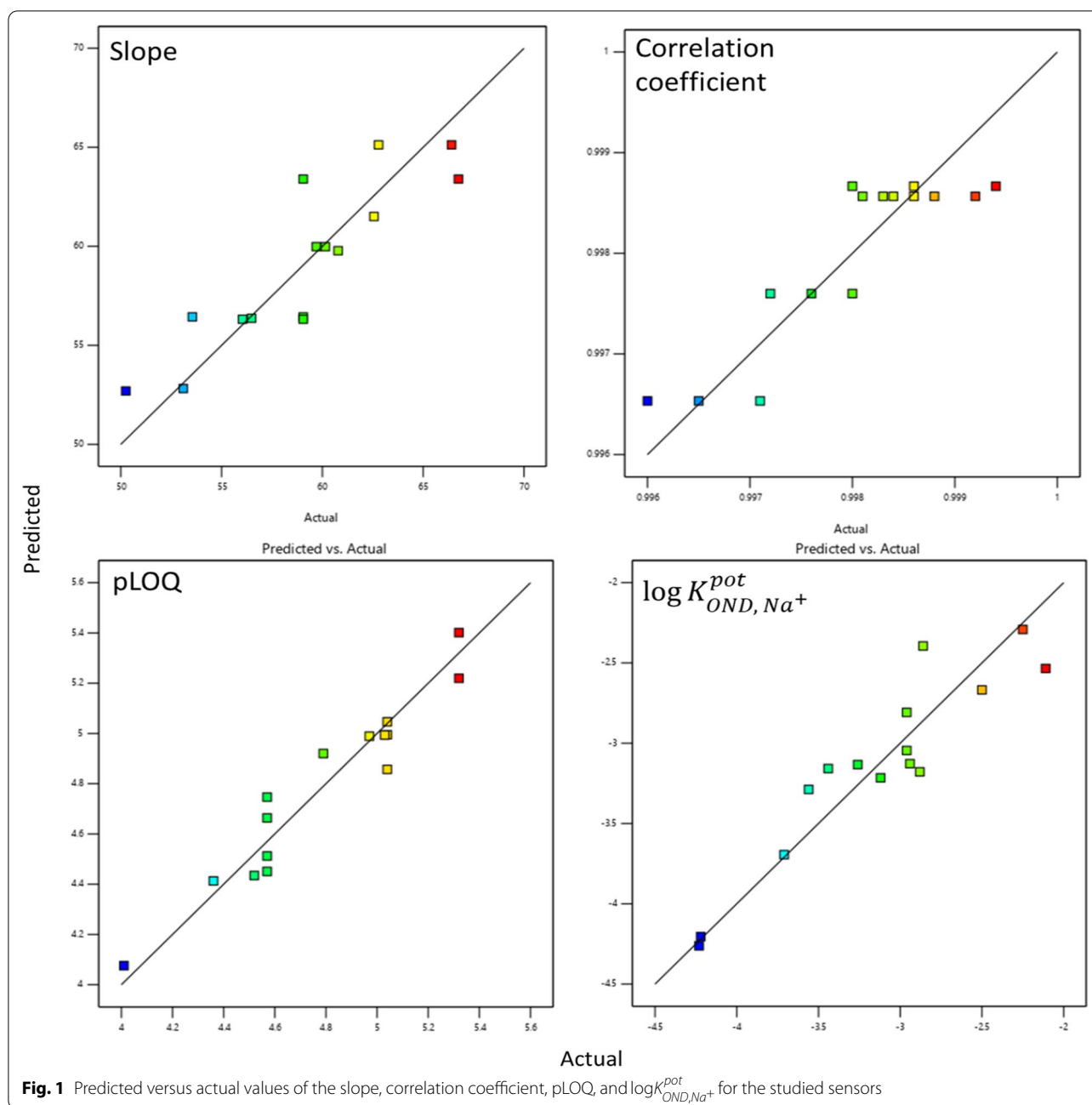
prevents co-extraction of similarly charged ions (Donnan exclusion effect), and selectively extracts the analyte ion from the sample solution. Its lipophilic nature minimizes loss due to leaching into the sample solution [54].

Ionophores are lipophilic molecules that bind selectively and reversibly to the analyte ion. It prevents efflux of the analyte ion and keeps its concentration constant within the membrane matrix. This minimizes potential perturbations and restricts potential changes to the change in the sample solution concentration [55].

We analyzed the results at five different ionophore levels (BCD, HPBCD, CMBCD, CX<sub>4</sub>, CX<sub>8</sub>). The ionophore type significantly affected the quantification limit and selectivity for sodium ions. Ionophores selectively recognize and reversibly bind the OND within the membrane matrix. Thus ionophores are lipophilic molecules that bind selectively and reversibly to the analyte ion. It prevents efflux of the analyte ion and keeps its concentration constant within the membrane matrix. This minimizes potential perturbations and restricts potential changes to the change in the sample solution concentration [51].

The program constructed four prediction models (one for each outcome). The predicted values were close to the actual values [56, 57], as shown in Fig. 1.

The desirability function used the built models to determine the optimal membrane composition according to the desired outcomes. We claimed a Nernstian slope,



maximum correlation coefficient, maximum pLOQ, and minimum sodium selectivity coefficient ( $\log K_{OND,Na}^{pot}$ ). The desirability function suggested the optimum membrane recipe. The recipe included NPOE as a plasticizer, TKS as an ion exchanger, and  $CX_4$  as an ionophore (Fig. 2). We constructed the suggested sensor and plotted the calibration graphs (Fig. 3). We compared the theoretical response parameters calculated by the software (slope = 59.99,  $r = 0.999$ , pLOQ = 5.401,  $\log K_{OND,Na}^{pot}$

= -2.96) with those obtained practically (slope = 60.23,  $r = 0.999$  and pLOQ = 5.401, and  $\log K_{OND,Na}^{pot} = -2.96$ ) to verify the model; the results were interestingly comparable.

#### Response characteristics of the optimized sensor

We followed the ICH guidelines [58] to validate the developed method (Accuracy, selectivity, precision etc.), as shown in Table 3. Whereas, the potentiometric

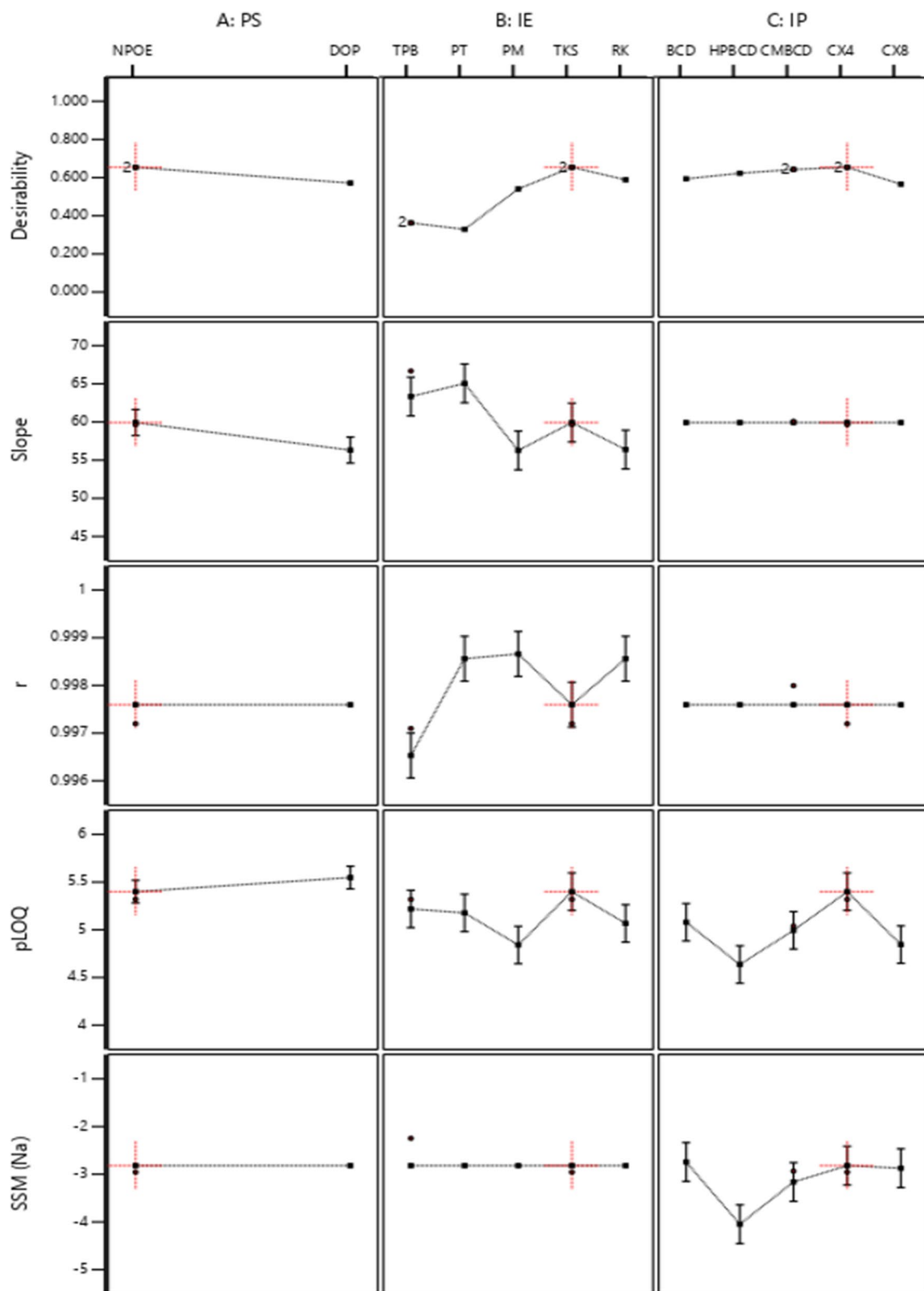
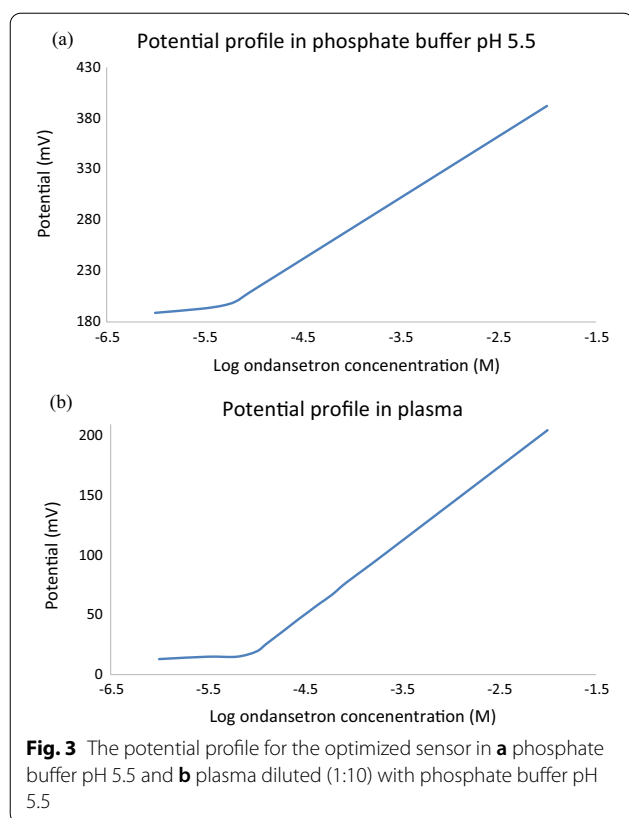


**Fig. 2** Results of the desirability function for the optimization of the sensor composition to achieve the desired optimum slope, maximum correlation coefficient, maximum pLOQ, and minimum  $\log K_{OND,Na}^{pot}$



sensor response parameters were evaluated according to the IUPAC guidelines [49], as shown in Table 3. The slope was calculated for the linear part of the potential-logarithm concentration relationship (Fig. 3). The optimized sensor displayed a Nernstian slope in phosphate buffer (60.23 mV/decade) and diluted plasma samples (61.90 mV/decade), as shown in Table 3. The detection

limit, quantification limit, correlation coefficient, and linear range are shown in Table 3.

The characteristics of the electrochemical response and validation parameters of OND analysis are shown in Table 3. The method's accuracy, repeatability, and intermediate precision were assessed at three different concentrations ( $1.0 \times 10^{-4}$ ,  $5.0 \times 10^{-4}$ , and  $1.0 \times 10^{-3}$  M) in phosphate buffer pH 5.5 and diluted plasma, as shown in Table 3. The sensor proved a stable potential response in pH 2–6, as shown in Table 3 and Fig. 4.

Below pH 6, the potential declined steeply. The decrease in the potential is attributed to a corresponding reduction in the charged OND species as the pH increases above its pKa value (7.34), and OND converts to the free basic form (uncharged). The optimized sensor equilibrates rapidly across the entire concentrations range resulting in a fast and stable response, as shown in Fig. 5. In addition, the sensor achieved more rapid equilibrium at higher OND concentrations (3 s) than at lower concentrations (6 s), as shown in Fig. 5 and Table 3.

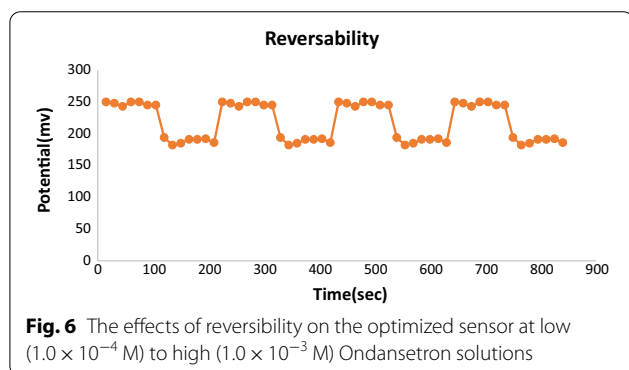
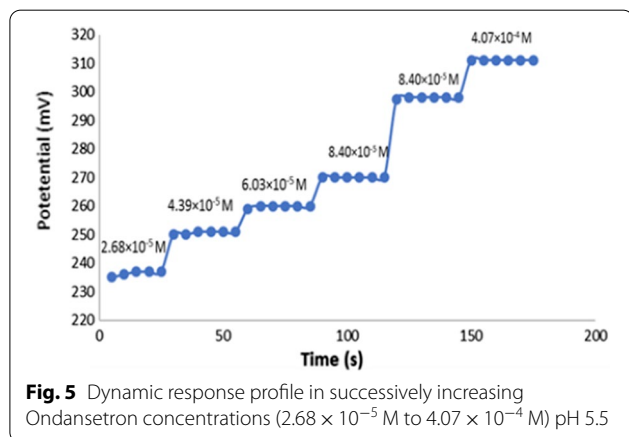
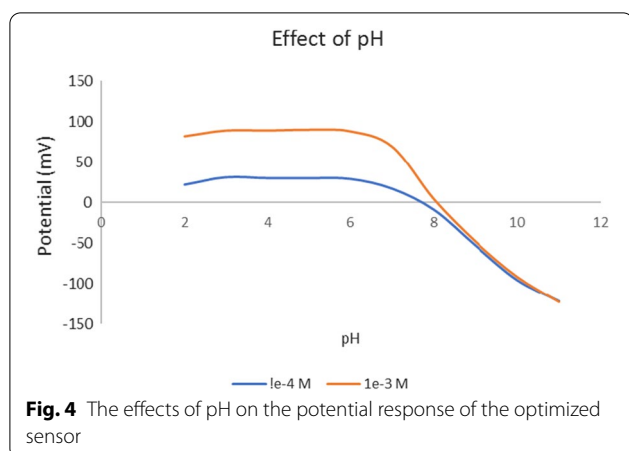
The sensor proved a stable slope  $\pm 1.0$  mV/decade for 4 weeks (Table 3). The loss in response is attributed to the leaching of membrane components from the PVC membrane. We calculated the quantification and detection limits according to the IUPAC recommendation. Results proved the sensor's capacity to detect OND in highly diluted solutions down to  $9.09 \times 10^{-6}$  M in phosphate buffer and  $1.00 \times 10^{-5}$  in human plasma (Table 3).

The performance of the suggested sensor may be utilized for 4 weeks without significantly changing. The reproducibility was evaluated by assessment of the reversibility of the sensor; the reversibility study expressed the fast OND exchange at the sensor sample interface, as shown in Fig. 6.

**Table 3** Validation parameters of the optimized sensor

Parameter	In phosphate buffer pH 5.5	In plasma
Linearity		
Slope (mV per decade)	60.23	61.90
Correlation coefficient (r)	0.999	0.998
Concentration range (M)	$9.09 \times 10^{-6}$ – $1.0 \times 10^{-2}$	$1.0 \times 10^{-5}$ – $1.0 \times 10^{-2}$
LOQ (M)	$9.09 \times 10^{-6}$	$1.00 \times 10^{-5}$
LOD (M)	$4.24 \times 10^{-6}$	$7.91 \times 10^{-6}$
Accuracy (mean $\pm$ SD)	100.05 $\pm$ 0.577	100.15 $\pm$ 0.516
Precision		
Repeatability (%RSD)	1.051	1.970
Intermediate precision (%RSD)	1.106	1.889
Working pH range	2–6	
Response time (s)	3–6	
Life span (weeks)	4	





The selectivity study performed using the separate solution method [59], expressed the sensor selectivity for OND in the presence of commonly interfering cationic species naturally present in physiological fluids with different ionic sizes, mobility, and lipophilicity (Table 4). The calculated selectivity coefficients ( $K_{OND,Int}^{pot}$ ) prove that interferences did not affect the performance of the

**Table 4** Potentiometric selectivity coefficients of the optimized sensor for different interfering ions calculated using the separate solution method (59)

Interfering compound	$K_{OND,Int}^{pot}$ *
Potassium	$4.33 \times 10^{-3}$
Sodium	$1.09 \times 10^{-3}$
Ammonium	$3.07 \times 10^{-3}$
Calcium	$2.73 \times 10^{-4}$
Magnesium	$5.30 \times 10^{-5}$
Cadmium	$1.20 \times 10^{-4}$
ferrous	$1.08 \times 10^{-4}$
chromium	$2.70 \times 10^{-4}$

\* Average of three determinations

working electrode and demonstrated the sensor capacity for plasma applications.

The optimized sensor was successfully applied to determine OND in Zofran<sup>®</sup> tablet and spiked human plasma without prior extraction, pretreatment, or derivatization operations (Table 5).

Results obtained for the analysis of OND were statistically compared with a reported HPLC method [41]. The calculated *t* and *F* values at a 95% confidence interval were less than the tabulated ones, revealing no significant difference between the developed and reported methods concerning accuracy and precision (Table 5).

Although the reported OND potentiometric sensor [46], showed a longer life span of 7 weeks, it sluggishly responded to OND (response time 18 s). The proposed sensor is based on a data-driven QbD approach based on a custom experimental design. Additionally, the sensor resulting from this approach expressed a relatively faster response for OND that suits real-time assay. Contrary to the reported sensor, the developed sensor is applicable for OND assay in plasma samples.

## Conclusions

The adopted quality by design approach employs a custom experimental design to develop and optimize a potentiometric sensor for OND assay. The sensor was designed to fit the desired analytical purpose. The sensor shows a Nernstian slope, high correlation coefficient, low quantification limit, and high selectivity for OND. The desirability function selected the optimal PVC membrane recipe to achieve optimal sensor performance. The potentiometric method was validated for OND assay in Zofran<sup>®</sup> tablets and human plasma samples. The sensor can be used for fast, direct, sensitive, and selective OND assay in quality control laboratories, clinical laboratories, and pharmacokinetic studies.

**Table 5** Statistical comparison of the developed potentiometric method to the reported HPLC method for determination of OND in Zofran® tablets form and plasma sample

Parameter	Zofran® Tablet		Spiked human plasma samples	
	Developed potentiometric method	Reported <sup>a</sup> HPLC method	Developed potentiometric method	Reported <sup>a</sup> HPLC method (41)
Mean	100.01	100.84	98.26	98.67
SD	1.082	0.86	2.227	2.875
Variance	1.171	0.740	4.960	8.266
n	6	6	6	6
Student's t-test <sup>b</sup>	1.471 (2.228) <sup>b</sup>		0.276 (2.228) <sup>b</sup>	
F value <sup>b</sup>	1.583 (7.146) <sup>b</sup>		1.667 (7.146) <sup>b</sup>	

<sup>a</sup> HPLC method using C18 column as the stationary phase and a mixture consisting of acetonitrile: 0.02 M sodium phosphate monobasic buffer (pH adjusted to 3.0 using phosphoric acid) in ratio (60:40, v/v) as a mobile phase. The mobile phase was pumped at a flowrate of 1.5 ml/min. UV detection was carried out at 305.0 nm [41]

<sup>b</sup> Values in parentheses are the corresponding tabulated two-tailed values at significance level  $\alpha = 0.05$

#### Author contributions

MAA: data curation, validation, investigation, resources, writing—original draft. SAA: validation, formal analysis, investigation, data curation, supervision, writing—review & editing, visualization. sally S. EM: validation, formal analysis, investigation, data curation, supervision, writing—review & editing, visualization. MRE: conceptualization, methodology, validation, formal analysis, investigation, data curation, supervision, review & editing, visualization. HEZ: conceptualization, methodology, validation, formal analysis, investigation, data curation, supervision, review & editing, visualization. ASS: conceptualization, methodology, validation, formal analysis, investigation, data curation, supervision, writing—review & editing, visualization. All authors read and approved the final manuscript.

#### Funding

Open access funding provided by The Science, Technology & Innovation Funding Authority (STDF) in cooperation with The Egyptian Knowledge Bank (EKB). This work wasn't funded by any third party.

#### Availability of data and materials

Datasets generated and/or analyzed during the current study are available from the corresponding author on reasonable request.

#### Declarations

##### Ethics approval and consent to participate

Not applicable.

##### Consent for publication

Not applicable.

##### Competing interests

The authors declare that they have no known competing financial interests or personal relationships that could have appeared to influence the work reported in this paper.

#### Author details

<sup>1</sup>Analytical Chemistry Department, Faculty of Pharmacy, October 6 University, 6 October City, PO box 12858, Giza, Egypt. <sup>2</sup>Pharmaceutical Chemistry Department, Egyptian Drug Authority, 51 Wezaret El-Zeraa St, Cairo, Egypt. <sup>3</sup>Analytical Chemistry Department, Faculty of Pharmacy, Cairo University, Kasr El-Aini St, PO 11562, Cairo, Egypt. <sup>4</sup>Medicinal Chemistry Department, PharmD program, Egypt-Japan University of Science and Technology (E-JUST), New Borg El-Arab City, PO 21934, Alexandria, Egypt.

Received: 28 May 2022 Accepted: 28 September 2022

Published online: 13 October 2022

#### References

- Lawrence XY, Amidon G, Khan MA, Hoag SW, Polli J, Raju G, Woodcock J. Understanding pharmaceutical quality by design. *AAPS J*. 2014;16(4):771–83.
- Beg S, Swain S, Rahman M, Hasnain MS, Imam SS. Application of design of experiments (DoE) in pharmaceutical product and process optimization. *Pharmaceutical quality by design*. Amsterdam: Elsevier; 2019. p. 43–64.
- Raman N, Mallu UR, Bapatu HR. Analytical quality by design approach to test method development and validation in drug substance manufacturing. *J Chem*. 2015. <https://doi.org/10.1155/2015/435129>.
- Saad AS, Ismail NS, Soliman M, Zaazaa HE. Validated stability-indicating RP-HPLC method for simultaneous determination of clorsulon and ivermectin employing plackett-burman experimental design for robustness testing. *J AOAC Int*. 2016;99(2):571–8.
- Zeng L, Helsing LM, Nampo FK, Wang Y, Yao L, Siemieniuk RA, Bretthauer M, Guyatt GH. How do cancer screening guidelines trade off benefits versus harms and burdens of screening? A systematic survey. *BMJ Open*. 2020;10(12):e038322.
- Bray F, Ren JS, Masuyer E, Ferlay J. Global estimates of cancer prevalence for 27 sites in the adult population in 2008. *Int J Cancer*. 2013;132(5):1133–45.
- Wang R, Han L, Dai W, Mo S, Xiang W, Li Q, Xu Y, Cai G. Cause of death for elders with colorectal cancer: a real-world data analysis. *J Gastrointest Oncol*. 2020;11(2):269.
- Ballatori E, Roila F. Impact of nausea and vomiting on quality of life in cancer patients during chemotherapy. *Health Qual Life Outcomes*. 2003;1(1):46.
- Loewen PS, Marra CA, Zed PJ. 5-HT<sub>3</sub> receptor antagonists vs traditional agents for the prophylaxis of postoperative nausea and vomiting. *Can J Anesth*. 2000;47(10):1008–18.
- National Center for Biotechnology Information. PubChem Compound Summary for CID 4595, Ondansetron. <https://pubchem.ncbi.nlm.nih.gov/compound/Ondansetron>. Accessed 11 Oct 2022.
- Roila F. Antiemetic Subcommittee of the Multinational Association of Supportive Care in Cancer (MASCC). Prevention of chemotherapy- and radiotherapy-induced emesis: results of the 2004 Perugia International Antiemetic Consensus Conference. *Ann Oncol*. 2006;17:20–8.
- Butcher M. Global experience with ondansetron and future potential. *Oncology*. 1993;50(3):191–7.

13. Joslyn A. Ondansetron, clinical development for postoperative nausea and vomiting: current studies and future directions. *Anaesthesia*. 1994;49:34–7.
14. Fischer V, Vickers A, Heitz F, Mahadevan S, Baldeck J, Minery P, Tynes R. The polymorphic cytochrome P-450D6 is involved in the metabolism of both 5-hydroxytryptamine antagonists, tropisetron and ondansetron. *Drug Metab Dispos*. 1994;22(2):269–74.
15. BP. *British Pharmacopoeia*, vol. II, 6<sup>th</sup> ed. The Stationary Office, London; 2009.
16. Prabu SLJA, Shirwaikar AA, Jeyaprakash RS. Spectrofluorimetric method for determination of granisetron hydrochloride in bulk and pharmaceutical dosage forms. *Indian Drugs*. 2008;45(563):6.
17. Deepshikh GSP. Development and validation of spectrophotometric method for determination of ondansetron hydrochloride in bulk and formulation. *JGPT*. 2013;1:6–10.
18. Hewala BM II, Shousha SM. First derivative spectrophotometric determination of granisetron hydrochloride in presence of its hydrolytic products and preservative and application to pharmaceutical preparations. *Drug Test Anal*. 2013;234(5):41.
19. Shetty AS, Poornima A, Ahmed M, Kumar S. Simultaneous estimation of esomeprazole and ondansetron in bulk and combined tablet dosage form by uv-spectrophotometric methods. *IJUPBS*. 2014;3:270–83.
20. Bourdon F, Lecoœur M, Odou P, Vaccher C, Foulon C. Complementarity of UV-PLS and HPLC for the simultaneous evaluation of antiemetic drugs. *Talanta*. 2014;120:274–82.
21. Prashanthi M, Venkateshwaralu G. Spectrophotometric estimation of drugs using N-Bromo succinamide and amaranth dye couple. *Int J Pharm Res Anal*. 2014;4:58–64.
22. Kumar PR, Krishna MM, Prakash PB, Kumar BA, Madhusudhan P. Derivative spectrophotometric estimation of ondansetron and paracetamol. *J Chem*. 2006;3(3):134–6.
23. Patra S, Choudhury A, Kar R, Barik B. Spectrophotometric method for ondansetron hydrochloride. *Indian J Pharm Sci*. 2007;69(6):840.
24. Sreedhar N, Sivaprasad M, Seenu N, Swarupa C, Dhananjayulu M. Determination of ondansetron HCL at hanging mercury drop electrode (HMDE) by electroanalytical techniques. *Int J Pharm Pharm Sci*. 2012;2:90–4.
25. Nigović B, Sadiković M, Sertić M. Multi-walled carbon nanotubes/Nafion composite film modified electrode as a sensor for simultaneous determination of ondansetron and morphine. *Talanta*. 2014;122:187–94.
26. Wring SA, Rooney RM, Goddard CP, Waterhouse I, Jenner WN. A sensitive radioimmunoassay, combined with solid-phase extraction, for the sub-nanogram per ml determination of ondansetron in human plasma. *J Pharm Biomed Anal*. 1994;12(3):361–71.
27. Zamora LL, Calatayud JM. Continuous flow-injection-atomic absorption spectrometric method for the determination of Ondansetron. *Anal Chim Acta*. 1995;300(1–3):143–8.
28. Wen-bing S. Flow-injection chemiluminescence analysis of granisetron hydrochloride with nanometer microreactor. *Chin J Anal Lab*. 2008;5:19.
29. Mujtaba A, Kohli K, Ali J, Baboota S. Development of HPTLC method for the estimation of ondansetron hydrochloride in bulk drug and sublingual tablets. *Drug Test Anal*. 2013;5(2):122–5.
30. Raval P, Puranik M, Wadher S, Yeole P. A validated HPTLC method for determination of ondansetron in combination with omeprazole or rabeprazole in solid dosage form. *Indian J Pharm Sci*. 2008;70(3):386.
31. Huang C, Wan H, Zhang J, Zhong H, Li J, Sun Y, Wang Q, Zhang H. Quantification of ondansetron, granisetron and tropisetron in goat plasma using hydrophilic interaction liquid chromatography-solid phase extraction coupled with hydrophilic interaction liquid chromatography-triple quadrupole tandem mass spectrometry. *J Chromatogr B*. 2018;1095:50–8.
32. Balint A, Silvia I, Bondoroi-Papp Z, Muntean D-L. Development of a new rp-hplc method for ondansetron determination in injectable formulations. *Med-Surg J*. 2018;122(1):207–12.
33. Chen F-c, Wang L-h, Guo J, Shi X-y, Fang B-x. Simultaneous determination of dexamethasone, ondansetron, granisetron, tropisetron, and azasetron in infusion samples by HPLC with DAD detection. *J Anal Methods Chem*. 2017. <https://doi.org/10.1155/2017/6749087>.
34. Atrey E, Shende P, Gaud R. RP-HPLC method development and validation for simultaneous estimation of ondansetron hydrochloride and complexed famotidine in bulk and dosage form. *J Anal Pharm Res*. 2017;5(2):00138.
35. Dedania Z, Dedania R, Karkhanis V, Sagar GV, Baldania M, Sheth N. RP-HPLC method for simultaneous estimation of omeprazole and ondansetron in combined dosage forms. *Asian J Res Chem*. 2009;2(2):108–11.
36. Meyyanathan S, Venkatesh DN, Krishnaveni N, Babu B, Jeyaprakash M, Raja RB, Hemnath E, Suresh B. A RP-HPLC method for simultaneous estimation of ondansetron and ranitidine in pharmaceutical formulation. *Int J Health Allied Sci*. 2012;1(2):129.
37. Patel SR, Patel L, Thakkar YP, Patel ND. Development and Validation of analytical method for the determination of Rabeprazole and Ondansetron in pharmaceutical dosage form by reversed-phase HPLC. *Int J Chem Tech Res*. 2010;2(3):1531–6.
38. Bauer S, Störmer E, Kaiser R, Tremblay PB, Brockmöller J, Roots I. Simultaneous determination of ondansetron and tropisetron in human plasma using HPLC with UV detection. *Biomed Chromatogr*. 2002;16(3):187–90.
39. Zheng H-S, Pan W, Wang Y, Mao S-R, Bi D-Z. Determination of ondansetron hydrochloride in human plasma by HPLC. *Chin J Pharm*. 2002;33(12):603–4.
40. Mohamed AMI, Mohamed NA-L. Development and validation of RP-HPLC method for simultaneous determination of ondansetron hydrochloride and granisetron hydrochloride in their admixtures with pantoprazole sodium. *Thai J Pharm Sci*. 2020;44(2):82–90.
41. Dépôt M, Leroux S, Caillé G. High-resolution liquid chromatographic method using ultraviolet detection for determination of ondansetron in human plasma. *J Chromatogr B Biomed Sci Appl*. 1997;693(2):399–406.
42. Abdel-Hamid ME, Sharma D. Simultaneous quantification of doxorubicin, lorazepam, metoclopramide, ondansetron, and ranitidine in mixtures by liquid chromatography-tandem mass spectrometry. *J Liq Chromatogr Relat Technol*. 2004;27(4):641–60.
43. Pang L, Wang Q, Wang Y, Zheng M, Wu H, Wang Z. Development and Validation of LC-MS/MS Method for Determination of Ondansetron in rat Plasma and its Application. *Latin American Journal of Pharmacy*. 2012; 31(2):305–309.
44. Abd El-Rahman MK, Zaazaa HE, Eidin NB, Moustafa AA. Just-dip-it (potentiometric ion-selective electrode): an innovative way of greening analytical chemistry. *ACS Sustain Chem Eng*. 2016;4(6):3122–32.
45. Gupta KV, Nayak A, Agarwal S, Singhal B. Recent advances on potentiometric membrane sensors for pharmaceutical analysis. *Comb Chem High Throughput Screen*. 2011;14(4):284–302.
46. Faridbod F, Mizani F, Ganjali MR, Norouzi P. Determination of ondansetron hydrochloride by a liquid membrane potentiometric sensor based on room temperature ionic liquids. *Int J Electrochem Sci*. 2013;8(8):10461–72.
47. Soliman SS, Sedik GA, Elghobashy MR, Zaazaa HE, Saad AS. Greenness assessment profile of a QbD screen-printed sensor for real-time monitoring of sodium valproate. *Microchem J*. 2022;182:107859.
48. Galal MM, Saad AS. Portable solid-state sensor for therapeutic monitoring of an antineoplastic drug; vinblastine in human plasma. *RSC Adv*. 2020;10(70):42699–705.
49. IUPAC. Recommendations for nomenclature of ion-selective electrodes (IUPAC recommendations 1994). *Pure Appl Chem*. 1994;66(12):2527–36.
50. Umezawa Y, Bühlmann P, Umezawa K, Tohda K, Amemiya S. Potentiometric selectivity coefficients of ion-selective electrodes. Part I. Inorganic cations (technical report). *Pure Appl Chem*. 2000;72(10):1851–2082.
51. Baumann EW. Trace fluoride determination with specific ion electrode. *Anal Chim Acta*. 1968;42:127–32.
52. Heragy MO, Mustafa A, Elzanfaly E, Saad AS. Portable solid-state potentiometric sensor based on polymeric ion-exchanger for the assay of the controversial food colorant (sunset yellow). *Anal Methods*. 2021;13:4896–903.
53. Bakker E, Bühlmann P, Pretsch E. Carrier-based ion-selective electrodes and bulk optodes. 1. General characteristics. *Chemical Reviews*. 1997;97(8):3083–132.
54. Kelani KM, Elzanfaly ES, Halim MK, Saad AS. Computational optimization of a novel solid-state sensor for stable assay of isoxsuprine hydrochloride in the presence of its nephrotoxic/hepatotoxic photothermal

degradation products: application in different sampling matrices. *New J Chem.* 2020;44(35):15260–9.

55. Bakker E, Pretsch E. Peer reviewed: the new wave of ion-selective electrodes. *Anal chem.* 2002;74(15):420–6.
56. Douglas C. *Montgomery—design and analysis of experiments.* Hoboken: Wiley; 2020.
57. Montgomery DC. *Design and analysis of experiments.* Hoboken: Wiley; 2020.
58. ICH, ICH Topic: Validation of analytical procedures: text and methodology: *Q2 (R1): 2005.* Published online 1–17.
59. Fry C, Langley S. *Ion-selective electrodes for biological systems.* London: CRC Press; 2002.

### Publisher's Note

Springer Nature remains neutral with regard to jurisdictional claims in published maps and institutional affiliations.

**Ready to submit your research? Choose BMC and benefit from:**

- fast, convenient online submission
- thorough peer review by experienced researchers in your field
- rapid publication on acceptance
- support for research data, including large and complex data types
- gold Open Access which fosters wider collaboration and increased citations
- maximum visibility for your research: over 100M website views per year

**At BMC, research is always in progress.**

Learn more [biomedcentral.com/submissions](https://biomedcentral.com/submissions)

